Universität Hamburg
DER FORSCHUNG | DER LEHRE | DER BILDUNG

ОРДЕНА ЛЕНИНА ИМ.М.В.КЕЛДЫША РАН

28th Texas Symposium on Relativistic Astrophysics

Novel Computational Methods for the Determination of Properties of Cosmic Magnetic Fields

Andrey Saveliev

University of Hamburg and Keldysh Institute for Applied Mathematics

December 16th, 2015

SPONSORED BY THE

Federal Ministry of Education and Research

Contents

EGMF – Various Constraints [Neronov and Semikoz, 2009]

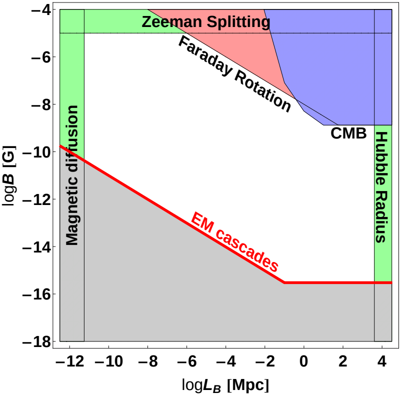

- Resistive decay due to magnetic diffusion removes short correlation lengths L_B

- L_B cannot be larger than the Hubble Radius
- EGMF cannot be stronger than galactic magnetic fields
- Non-observation of intergalactic Faraday Rotation for radio emisson from Quasars
- Non-observation of large scale angular anisotropies of the CMB
- Lower bound on B from gamma ray observations?

EGMF – Lower Bound on B?

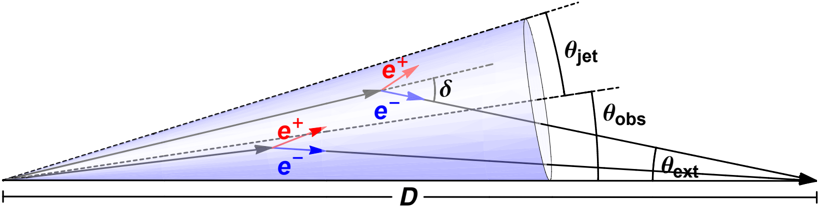

Gamma rays emitted from a blazar develop an electromagnetic cascade due to interactions with the Extragalactic Background Light (EBL) via Pair Production and Inverse Compton (IC) scattering. The interaction of this cascade with the EGMF results in several observational features. For example: Point-like sources appear extensive [Dolag et al., 2009], [Neronov et al., 2010]

GRPropa

- There are various propagation codes of electromagnetic cascades in the IGM (e.g. ELMAG [Kachelrieß et al., 2012]), however the simulations run in 1D, mimicking 3D effects (in particuar deflections due to magnetic fields) using the small-angle approximation

GRPropa

- There are various propagation codes of electromagnetic cascades in the IGM (e.g. ELMAG [Kachelrieß et al., 2012]), however the simulations run in 1D, mimicking 3D effects (in particular deflections due to magnetic fields) using the small-angle approximation
- GRPropa is a new software based on CRPropa 3.0 [Alves Batista et al., 2013] which is a full 3D Monte Carlo simuation including effects due to magnetic fields and cosmology

GRPropa

- There are various propagation codes of electromagnetic cascades in the IGM (e.g. ELMAG [Kachelrieß et al., 2012]), however the simulations run in 1D, mimicking 3D effects (in particuar deflections due to magnetic fields) using the small-angle approximation
- GRPropa is a new software based on CRPropa 3.0 [Alves Batista et al., 2013] which is a full 3D Monte Carlo simuation including effects due to magnetic fields and cosmology
- For a thorough analysis different EBL models for both Pair Production and Inverse Compton scattering are implemented

GRPropa – Comparison with ELMAG

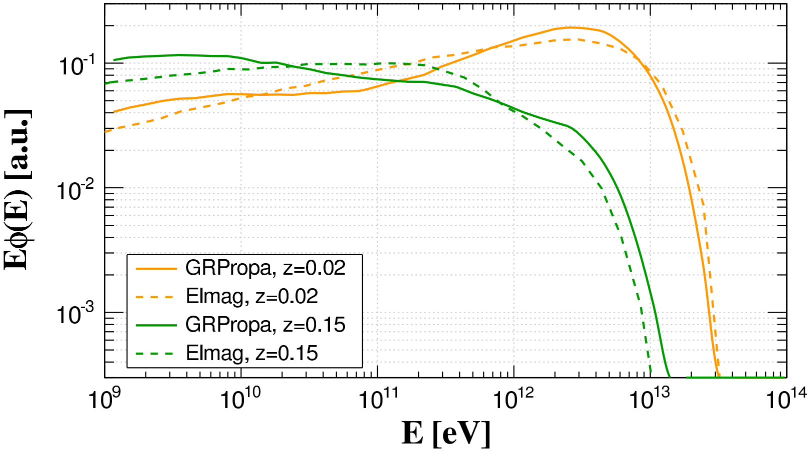

GRPropa – Magnetic fields

An important feature of GRPropa is the full implementation of magnetic fields. As input one can set their

- field strength B,

GRPropa – Magnetic fields

An important feature of GRPropa is the full implementation of magnetic fields. As input one can set their

- field strength B,
- configuration (presently: homogeneous or turbulent with a givenspectrum),

GRPropa – Magnetic fields

An important feature of GRPropa is the full implementation of magnetic fields. As input one can set their

- field strength B,
- configuration (presently: homogeneous or turbulent with a givenspectrum),
- coherence length,

GRPropa – Magnetic fields

An important feature of GRPropa is the full implementation of magnetic fields. As input one can set their

- field strength B,
- configuration (presently: homogeneous or turbulent with a givenspectrum),
- coherence length,
- helicity (in terms of the maximal value with a positive/negative sign).

GRPropa Results: Arrival Directions

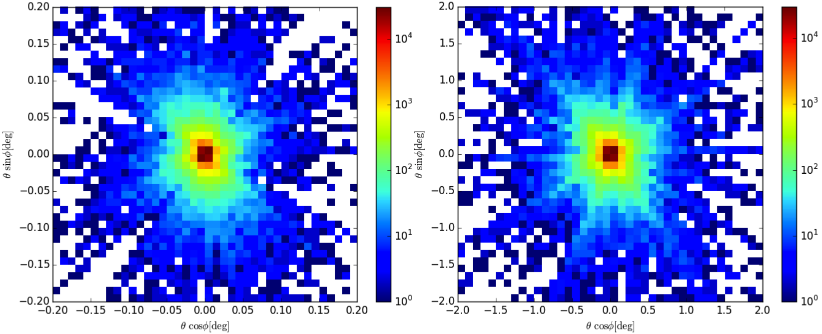

Gamma ray arrival directions ($10^{10}\,\mathrm{eV} \leq E_\gamma \leq 10^{11}\,\mathrm{eV}$) for a source at a distance $D = 1000\,\mathrm{Mpc}$ and energy dependence of the deflection for $B = 10^{-16}\,\mathrm{G}$ (left) and $B = 10^{-15}\,\mathrm{G}$ (right).

GRPropa Results: Energy Dependence of the Defl. Angle

$$\theta(E_\gamma) \simeq \frac{0.05^{\rm o}\kappa}{(1+z_{\rm s})^4}\left(\frac{B}{10^{-15}{\rm G}}\right)\left(\frac{E_\gamma}{100\,{\rm GeV}}\right)^{-1}\left(\frac{D_{\rm s}}{1\,{\rm Gpc}}\right)\left(\frac{E_{\rm TeV}}{10\,{\rm TeV}}\right)^{-1}$$

[Neronov and Semikoz, 2009]

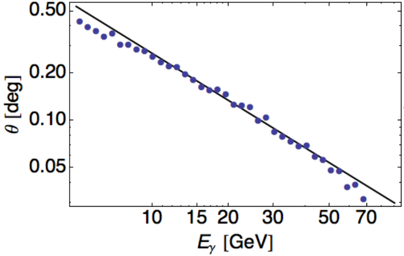

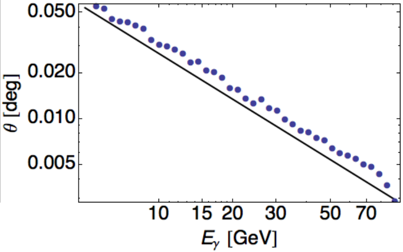

Dependence of the deflection angle θ on arrival energy E_γ for a monochromatic source ($E_{\rm TeV} = 10\,{\rm TeV}$) at a distance $D_{\rm s} = 1\,{\rm Gpc}$ for $B = 10^{-15}\,{\rm G}$ (left) and $B = 10^{-16}\,{\rm G}$ (right).

Directional Analysis

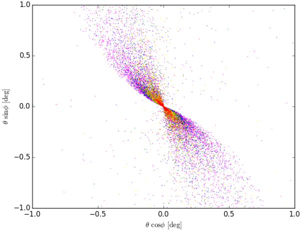

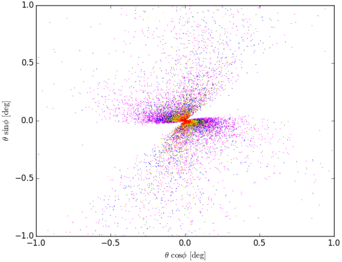

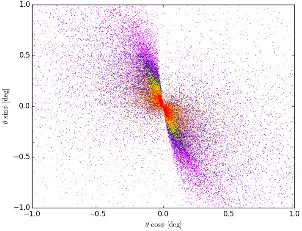

Sky maps for maximally negative and positive helicity (left) and no helicity (top), $B = 10^{-15}\,\mathrm{G}$, $L_B \simeq 225\,\mathrm{Mpc}$.

Directional Analysis

- Clear imprint of helicity on the arrival directions of gamma rays – analysis tool needed.

Directional Analysis

- Clear imprint of helicity on the arrival directions of gamma rays – analysis tool needed.
- Possible approach: Q statistics [Tashiro and Vachaspati, 2013, Tashiro et al., 2013]

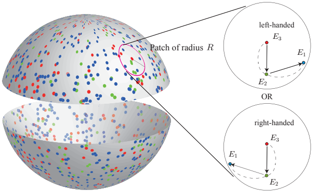

$$Q(E_1, E_2, E_3, R) = \frac{1}{N_3} \sum_{j=1}^{N_3} [\eta_1(R) \times \eta_2(R)] \cdot \mathbf{n}_j(E_3)\,,$$

where

$$\eta_a(R) \equiv \sum_{i \in \{i | \measuredangle(\mathbf{n}_i, \mathbf{n}_j) < R\}}^{N_a} \mathbf{n}_i(E_a)\,,$$

Directional Analysis

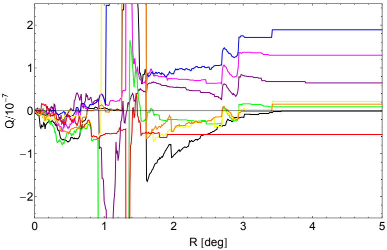

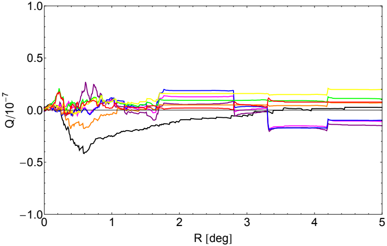

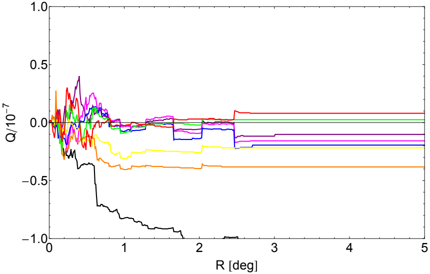

Q statistics for maximally negative and positive helicity (left) and no helicity (top), $B = 10^{-16}\,\mathrm{G}$, $L_B \simeq 225\,\mathrm{Mpc}$.

EGMF - Origin

The origin of EGMF is still uncertain – mainly two different concepts:

EGMF - Origin

The origin of EGMF is still uncertain – mainly two different concepts:

- Astrophysical scenario: Seed magnetic fields are generated during structure formation (e.g. by a Biermann Battery [Biermann, 1950]) and are then amplified by the dynamo effect [Zeldovich et al., 1980]

EGMF - Origin

The origin of EGMF is still uncertain – mainly two different concepts:

- Astrophysical scenario: Seed magnetic fields are generated during structure formation (e.g. by a Biermann Battery [Biermann, 1950]) and are then amplified by the dynamo effect [Zeldovich et al., 1980]
- Cosmological scenario: Strong seed magnetic fields are generated in the Early Universe, e.g. at a phase transition (QCD, electroweak) [Sigl et al., 1997] or during inflation [Turner and Widrow, 1988], and some of the initial energy content is transfered to larger scales.

EGMF - Origin

The origin of EGMF is still uncertain – mainly two different concepts:

- Astrophysical scenario: Seed magnetic fields are generated during structure formation (e.g. by a Biermann Battery [Biermann, 1950]) and are then amplified by the dynamo effect [Zeldovich et al., 1980]
- Cosmological scenario: Strong seed magnetic fields are generated in the Early Universe, e.g. at a phase transition (QCD, electroweak) [Sigl et al., 1997] or during inflation [Turner and Widrow, 1988], and some of the initial energy content is transfered to larger scales.

The latter are the so-called Primordial Magnetic Fields and will be focused on in the following.

EGMF - Origin

The origin of EGMF is still uncertain – mainly two different concepts:

- Astrophysical scenario: Seed magnetic fields are generated during structure formation (e.g. by a Biermann Battery [Biermann, 1950]) and are then amplified by the dynamo effect [Zeldovich et al., 1980]
- Cosmological scenario: Strong seed magnetic fields are generated in the Early Universe, e.g. at a phase transition (QCD, electroweak) [Sigl et al., 1997] or during inflation [Turner and Widrow, 1988], and some of the initial energy content is transfered to larger scales.

The latter are the so-called Primordial Magnetic Fields and will be focused on in the following.

- Basics for the time evolution: Homogeneous and isotropic magnetohydrodynamics in an expanding Universe.

Primordial Magnetic fields – Spectral Quantities

The aspect of interest is the distribution of energies on different scales k, i.e. the magnetic spectral energy density M of the magnetic fields and the kinetic magnetic spectral energy density U

$$\epsilon_B = \frac{1}{8\pi V}\int \mathbf{B}^2(\mathbf{x})\,\mathrm{d}^3x = \int \frac{|\hat{\mathbf{B}}(\mathbf{k})|^2}{8\pi}\mathrm{d}^3k \equiv \rho\int M_k \mathrm{d}k$$

$$\epsilon_K = \frac{\rho}{2V}\int \mathbf{v}^2(\mathbf{x})\,\mathrm{d}^3x = \frac{\rho}{2}\int |\hat{\mathbf{v}}(\mathbf{k})|^2\mathrm{d}^3k \equiv \rho\int U_k \mathrm{d}k$$

Primordial Magnetic fields – Spectral Quantities

The aspect of interest is the distribution of energies on different scales k, i.e. the magnetic spectral energy density M of the magnetic fields and the kinetic magnetic spectral energy density U

$$\epsilon_B = \frac{1}{8\pi V}\int \mathbf{B}^2(\mathbf{x})\,\mathrm{d}^3x = \int \frac{|\hat{\mathbf{B}}(\mathbf{k})|^2}{8\pi}\mathrm{d}^3k \equiv \rho \int M_k \mathrm{d}k$$

$$\epsilon_K = \frac{\rho}{2V}\int \mathbf{v}^2(\mathbf{x})\,\mathrm{d}^3x = \frac{\rho}{2}\int |\hat{\mathbf{v}}(\mathbf{k})|^2\mathrm{d}^3k \equiv \rho \int U_k \mathrm{d}k$$

In addition, for magnetic helicity one can define the spectral helicity density $\mathcal{H}$ by

$$h_B = \frac{1}{V}\int \mathbf{A}(\mathbf{x})\cdot\mathbf{B}(\mathbf{x})\,\mathrm{d}^3x = i\int\left(\frac{\mathbf{k}}{k^2}\times\hat{\mathbf{B}}(\mathbf{k})\right)\cdot\hat{\mathbf{B}}(\mathbf{k})^*\mathrm{d}^3k$$

$$\equiv \rho\int \mathcal{H}_k \mathrm{d}k$$

Primordial Magnetic Fields - Correlation Function

Aim: Computation of the correlation function for B and v

Aim: Computation of the correlation function for B and v

- Homogeneity: The correlation function cannot depend on the position in space

Primordial Magnetic Fields - Correlation Function

Aim: Computation of the correlation function for B and v

- Homogeneity: The correlation function cannot depend on the position in space
- Isotropy: The correlation function only depends on the magnitude of the spatial separation

Primordial Magnetic Fields - Correlation Function

Aim: Computation of the correlation function for B and v

- Homogeneity: The correlation function cannot depend on the position in space
- Isotropy: The correlation function only depends on the magnitude of the spatial separation

In Fourier space this means that the most general Ansatz is [von Kármán and Howarth, 1938, Junklewitz and Enßlin, 2011]

$$\langle \hat{B}_l(\mathbf{k}) \hat{B}_m(\mathbf{k}') \rangle \sim \delta(\mathbf{k} - \mathbf{k}')[(\delta_{lm} - \frac{k_l k_m}{k^2}) M(k) - \frac{i}{8\pi} \epsilon_{lmj} k_j \mathcal{H}(k)]$$

$$\langle \hat{v}_l(\mathbf{k}) \hat{v}_m(\mathbf{k}') \rangle \sim \delta(\mathbf{k} - \mathbf{k}')[(\delta_{lm} - \frac{k_l k_m}{k^2}) U(k) - \frac{i\rho}{2k^2} \epsilon_{lmj} k_j \mathcal{H}^{\mathrm{K}}(k)]$$

Master Equations for the Time Evolution of M, U and $\mathcal{H}$

$$
\langle \partial_t M_q \rangle = \int_0^\infty \Bigg(\Delta t \Bigg\{ -\frac{2}{3} q^2 \langle M_q \rangle \langle U_k \rangle - \frac{4}{3} q^2 \langle M_q \rangle \langle M_k \rangle + \frac{1}{3} \frac{1}{(4\pi)^2} q^2 k^2
$$

$$
+ \int_0^\pi \left[\frac{1}{2} \frac{q^4}{k_1^4} \left(q^2 + k^2 - qk\cos\theta \right) \sin^3\theta \, \langle M_k \rangle \langle U_{k_1} \rangle \right] \mathrm{d}\theta \Bigg\} \Bigg) \mathrm{d}k
$$

$$
\left\langle \partial_t U_q \right\rangle = \int_0^\infty \Bigg(\Delta t \Bigg\{ -\frac{2}{3} q^2 \langle M_k \rangle \left\langle U_q \right\rangle - \frac{2}{3} q^2 \left\langle U_q \right\rangle \langle U_k \rangle
$$

$$
+ \int_0^\pi \Bigg[\frac{1}{4} \frac{q^3 k}{k_1^4} \left(qk\sin^2\theta + 2k_1^2 \cos\theta \right) \sin\theta \, \langle M_k \rangle \left\langle M_{k_1} \right\rangle + \frac{1}{4} \frac{q^4 k}{k_1^4} \left(3k - q\cos\theta \right) \sin^3\theta \, \langle U_k \rangle \left\langle U_{k_1} \right\rangle
$$

$$
+ \frac{1}{(16\pi)^2} \frac{q^3 k^2}{k_1^2} \left(-2q - q\sin^2\theta + 2k\cos\theta \right) \sin\theta \, \langle \mathcal{H}_k \rangle \left\langle \mathcal{H}_{k_1} \right\rangle \Bigg] \mathrm{d}\theta \Bigg\} \Bigg) \mathrm{d}k
$$

$$
\langle \partial_t \mathcal{H}_q \rangle = \int_0^\infty \Bigg\{ \Delta t \Bigg[\frac{4}{3} k^2 \langle M_q \rangle \langle \mathcal{H}_k \rangle - \frac{4}{3} q^2 \langle M_k \rangle \langle \mathcal{H}_q \rangle
$$

$$
- \frac{2}{3} q^2 \langle U_k \rangle \langle \mathcal{H}_q \rangle + \int_0^\pi \left(\frac{1}{2} \frac{q^4 k^2}{k_1^4} \sin^3\theta \left\langle U_{k_1} \right\rangle \langle \mathcal{H}_k \rangle \right) \mathrm{d}\theta \Bigg] \Bigg\} \mathrm{d}k
$$

Definitions:

$\mathbf{k_1} \equiv \mathbf{q} - \mathbf{k}$

$\mathbf{q} \cdot \mathbf{k} \equiv qk\cos\theta$

Energy/helicity conservation: $\partial_t \epsilon_{\mathrm{tot}} = \rho \int \left(\partial_t M_q + \partial_t U_q \right) \mathrm{d}q = 0$ and $\partial_t h_{\mathrm{B}} = \rho \int \partial_t \mathcal{H}_q \mathrm{d}q = 0$

Results on the Time Evolution of Primordial Magnetic Fields without Helicity

[Saveliev et al., 2012]

- Starting either with an initial power-law ...

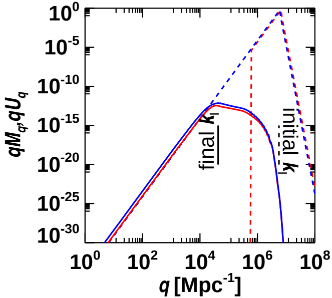

Results on the Time Evolution of Primordial Magnetic Fields without Helicity

[Saveliev et al., 2012]

- Starting either with an initial power-law ...
- ... or a concentration of the spectral energies on a single scale the qualitative result is similar: a tendence to equipartition and both $M_q \propto q^4 \propto L^{-4}$ (i.e. $B \propto q^{\frac{5}{2}} \propto L^{-\frac{5}{2}}$) and $U_q \propto q^4$ at large scales.

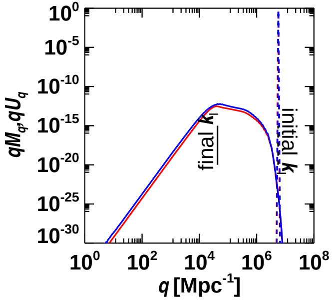

Results on the Time Evolution of Primordial Magnetic Fields without Helicity

- Starting either with an initial power-law ...
- ... or a concentration of the spectral energies on a single scale the qualitative result is similar: a tendence to equipartition and both $M_q \propto q^4 \propto L^{-4}$ (i.e. $B \propto q^{\frac{5}{2}} \propto L^{-\frac{5}{2}}$) and $U_q \propto q^4$ at large scales.

[Saveliev et al., 2012]

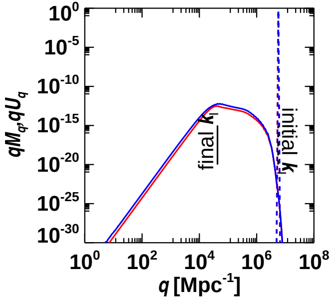

- A rough estimate for B (for the QCD phase transition) is given by $B(200\,\mathrm{pc}) \lesssim 5 \times 10^{-12}\,\mathrm{G}$

Results on the Time Evolution of Primordial Magnetic Fields with Helicity

- Including magnetic helicity for the same initial conditions results in an Inverse Cascade, a fast transport of big amounts of magnetic energy to large scales. This is due to helicity conservation.

[Saveliev et al., 2013]

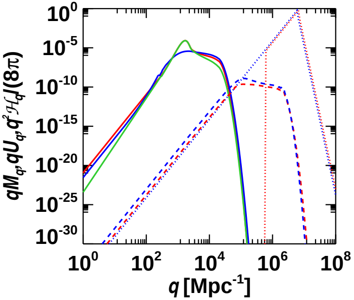

Results on the Time Evolution of Primordial Magnetic Fields with Helicity

- Including magnetic helicity for the same initial conditions results in an Inverse Cascade, a fast transport of big amounts of magnetic energy to large scales. This is due to helicity conservation.

[Saveliev et al., 2013]

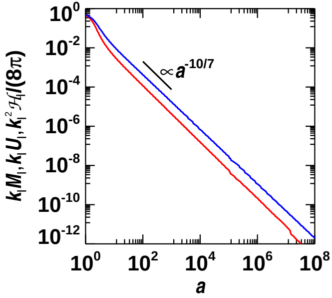

  - Two regimes are visible: When helicity is small, the considerations of the non-helical case are valid; once helicity reaches its maximal value, the behaviour changes dramatically

Results on the Time Evolution of Primordial Magnetic Fields with Helicity

[Saveliev et al., 2013]

- Including magnetic helicity for the same initial conditions results in an Inverse Cascade, a fast transport of big amounts of magnetic energy to large scales. This is due to helicity conservation.

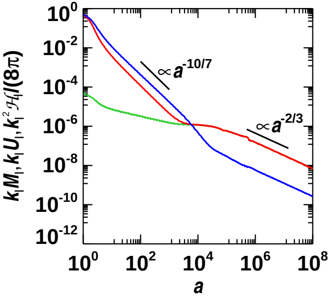

  - Two regimes are visible: When helicity is small, the considerations of the non-helical case are valid; once helicity reaches its maximal value, the behaviour changes dramatically

Boltzmann Equation

The time evolution of the distribution function is governed by the Boltzmann Equation which reads (without external forces)

$$\partial_t f(\mathbf{x}, \boldsymbol{\xi}, t) + \boldsymbol{\xi} \cdot \nabla f(\mathbf{x}, \boldsymbol{\xi}, t) = C(f)$$

On the right hand side $C(f)$ is the so-called Collision Integral which describes the interaction between particles and which is usually highly non-linear.

Boltzmann Equation

The time evolution of the distribution function is governed by the Boltzmann Equation which reads (without external forces)

$$\partial_t f(\mathbf{x}, \boldsymbol{\xi}, t) + \boldsymbol{\xi} \cdot \nabla f(\mathbf{x}, \boldsymbol{\xi}, t) = C(f)$$

On the right hand side $C(f)$ is the so-called Collision Integral which describes the interaction between particles and which is usually highly non-linear.
This prevents analytical solutions, but at equilibrium it is $C(f) = 0$ and f is Maxwellian:

$$f_{\mathrm{M}}(\mathbf{x}, \boldsymbol{\xi}, t) = \frac{\rho(\mathbf{x}, t) m^{\frac{1}{2}}}{[2k_{\mathrm{B}} T(\mathbf{x}, t)]^{\frac{3}{2}}} \exp\left\{-\frac{m}{2k_{\mathrm{B}} T} [\boldsymbol{\xi} - \mathbf{v}(\mathbf{x}, t)]^2\right\}$$

The Kinetic Consistent Scheme

The starting point is the Maxwellian distribution function f_{M}, i.e. $C(f) = 0$. After a short time τ, up to the second order, one gets the Taylor Expansion

$$f(\mathbf{x}, \boldsymbol{\xi}, t + \tau) \simeq f_{\mathrm{M}}(\mathbf{x}, \boldsymbol{\xi}, t) + \tau \partial_t f_{\mathrm{M}}(\mathbf{x}, \boldsymbol{\xi}, t) + \frac{\tau^2}{2} \partial_t^2 f_{\mathrm{M}}(\mathbf{x}, \boldsymbol{\xi}, t)\,,$$

The Kinetic Consistent Scheme

The starting point is the Maxwellian distribution function f_{M}, i.e. $C(f) = 0$. After a short time τ, up to the second order, one gets the Taylor Expansion

$$f(\mathbf{x}, \boldsymbol{\xi}, t + \tau) \simeq f_{\mathrm{M}}(\mathbf{x}, \boldsymbol{\xi}, t) + \tau \partial_t f_{\mathrm{M}}(\mathbf{x}, \boldsymbol{\xi}, t) + \frac{\tau^2}{2} \partial_t^2 f_{\mathrm{M}}(\mathbf{x}, \boldsymbol{\xi}, t)\,,$$

which, using the Boltzmann Equation, becomes

$$\begin{aligned} f(\mathbf{x}, \boldsymbol{\xi}, t + \tau) \simeq{}& f_{\mathrm{M}}(\mathbf{x}, \boldsymbol{\xi}, t) - \tau \left(\boldsymbol{\xi} \cdot \nabla\right) f_{\mathrm{M}}(\mathbf{x}, \boldsymbol{\xi}, t) \\ &+ \frac{\tau^2}{2} \left(\boldsymbol{\xi} \cdot \nabla\right) \left(\boldsymbol{\xi} \cdot \nabla\right) f_{\mathrm{M}}(\mathbf{x}, \boldsymbol{\xi}, t)\,, \end{aligned}$$

The Kinetic Consistent Scheme

The starting point is the Maxwellian distribution function f_{M}, i.e. $C(f) = 0$. After a short time τ, up to the second order, one gets the Taylor Expansion

$$f(\mathbf{x}, \boldsymbol{\xi}, t+\tau) \simeq f_{\mathrm{M}}(\mathbf{x}, \boldsymbol{\xi}, t) + \tau \partial_t f_{\mathrm{M}}(\mathbf{x}, \boldsymbol{\xi}, t) + \frac{\tau^2}{2} \partial_t^2 f_{\mathrm{M}}(\mathbf{x}, \boldsymbol{\xi}, t)\,,$$

which, using the Boltzmann Equation, becomes

$$\begin{aligned} f(\mathbf{x}, \boldsymbol{\xi}, t+\tau) \simeq {} & f_{\mathrm{M}}(\mathbf{x}, \boldsymbol{\xi}, t) - \tau\,(\boldsymbol{\xi} \cdot \nabla)\, f_{\mathrm{M}}(\mathbf{x}, \boldsymbol{\xi}, t) \\ & + \frac{\tau^2}{2}\,(\boldsymbol{\xi} \cdot \nabla)\,(\boldsymbol{\xi} \cdot \nabla)\, f_{\mathrm{M}}(\mathbf{x}, \boldsymbol{\xi}, t)\,, \end{aligned}$$

or

$$\begin{aligned} & \frac{f(\mathbf{x}, \boldsymbol{\xi}, t+\tau) - f_{\mathrm{M}}(\mathbf{x}, \boldsymbol{\xi}, t)}{\tau} + (\boldsymbol{\xi} \cdot \nabla)\, f_{\mathrm{M}}(\mathbf{x}, \boldsymbol{\xi}, t) \\ & \simeq \frac{\tau}{2}\,(\boldsymbol{\xi} \cdot \nabla)\,(\boldsymbol{\xi} \cdot \nabla)\, f_{\mathrm{M}}(\mathbf{x}, \boldsymbol{\xi}, t)\,, \end{aligned}$$

Integrating this equation with the same invariants as above gives the corresponding time evolution equation, for example with $\int m\boldsymbol{\xi} \ldots \mathrm{d}^3\xi$:

$$
\begin{aligned}
&\partial_t \left(\rho v_i\right) + \partial_k \left(p\delta_{ik} + \rho v_i v_k\right) \\
&= \frac{\tau}{2}\partial_k \left[\partial_l \left(p v_k \delta_{il} + p v_l \delta_{ik} + p v_i \delta_{kl} + \rho v_i v_k v_l\right)\right]
\end{aligned}
$$

The Kinetic Consistent Scheme

Integrating this equation with the same invariants as above gives the corresponding time evolution equation, for example with $\int m\boldsymbol{\xi} ... \mathrm{d}^3\xi$:

$$
\begin{aligned}
&\partial_t \left(\rho v_i\right) + \partial_k \left(p\delta_{ik} + \rho v_i v_k\right) \\
&= \frac{\tau}{2}\partial_k \left[\partial_l \left(p v_k \delta_{il} + p v_l \delta_{ik} + p v_i \delta_{kl} + \rho v_i v_k v_l\right)\right]
\end{aligned}
$$

Identifying τ with the relaxation time, one gets the Navier-Stokes-Equations with all dissipative terms from first principles, without the necessity of their *ad hoc*-introduction (as done usually).

The Kinetic Consistent Scheme

Integrating this equation with the same invariants as above gives the corresponding time evolution equation, for example with $\int m\boldsymbol{\xi}\ldots\mathrm{d}^3\xi$:

$$\begin{aligned}&\partial_t\left(\rho v_i\right)+\partial_k\left(p\delta_{ik}+\rho v_i v_k\right)\\&=\frac{\tau}{2}\partial_k\left[\partial_l\left(pv_k\delta_{il}+pv_l\delta_{ik}+pv_i\delta_{kl}+\rho v_i v_k v_l\right)\right]\end{aligned}$$

Identifying τ with the relaxation time, one gets the Navier-Stokes-Equations with all dissipative terms from first principles, without the necessity of their *ad hoc*-introduction (as done usually).
This time evolution equation for ρv_i (as well as the others for ρ and ϵ_{tot}) can be written in the general symbolic form $\partial_t\left(\rho v_i\right)+\nabla\cdot\boldsymbol{\Phi}=0$, i.e. a continuity equation with flux $\boldsymbol{\Phi}$.

Therefore the following algorithm for the time evolution is applied [Chetverushkin, 2008]:

- At time t^j the distribution function in each computational cell centered around $\mathbf{x}_i$ is Maxwellian,
  i.e. $f(\mathbf{x}_i, \boldsymbol{\xi}, t^j) = f_{\mathrm{M}}(\mathbf{x}_i, \boldsymbol{\xi}, t^j)$

The Kinetic Consistent Scheme

Therefore the following algorithm for the time evolution is applied [Chetverushkin, 2008]:

- At time t^j the distribution function in each computational cell centered around $\mathbf{x}_i$ is Maxwellian, i.e. $f(\mathbf{x}_i, \boldsymbol{\xi}, t^j) = f_{\mathrm{M}}(\mathbf{x}_i, \boldsymbol{\xi}, t^j)$
- Over the time $[t^j,\ t^{j+1} = t^j + \tau]$ collisionless evolution takes place, the fluxes for each quantity are calculated, such that the new values may be obtained for each cell

The Kinetic Consistent Scheme

Therefore the following algorithm for the time evolution is applied [Chetverushkin, 2008]:

- At time t^j the distribution function in each computational cell centered around $\mathbf{x}_i$ is Maxwellian, i.e. $f(\mathbf{x}_i, \boldsymbol{\xi}, t^j) = f_{\mathrm{M}}(\mathbf{x}_i, \boldsymbol{\xi}, t^j)$
- Over the time $[t^j,\ t^{j+1} = t^j + \tau]$ collisionless evolution takes place, the fluxes for each quantity are calculated, such that the new values may be obtained for each cell
- At time $t = t^{j+1}$ the distribution function is instantly Maxwellized and the procedure is repeated for the next time step

The Kinetic Consistent Scheme

Therefore the following algorithm for the time evolution is applied [Chetverushkin, 2008]:

- At time t^j the distribution function in each computational cell centered around $\mathbf{x}_i$ is Maxwellian,
  i.e. $f(\mathbf{x}_i, \boldsymbol{\xi}, t^j) = f_{\mathrm{M}}(\mathbf{x}_i, \boldsymbol{\xi}, t^j)$
- Over the time $[t^j,\ t^{j+1} = t^j + \tau]$ collisionless evolution takes place, the fluxes for each quantity are calculated, such that the new values may be obtained for each cell
- At time $t = t^{j+1}$ the distribution function is instantly Maxwellized and the procedure is repeated for the next time step

But what about magnetic fields?

Application: Outflow of Matter from Galaxies

The Kinetic Consistent Scheme

Implementation of magnetic fields is rather difficult due to their pseudo-vector character. Only recently [Chetverushkin et al., 2013],[Chetverushkin et al., 2014] this has been possible by extending the velocity vector $\mathbf{v}$ to the complex plane, $\mathbf{v} \to \mathbf{v} + i\mathbf{v}_{\mathrm{A}}$, where $\mathbf{v}_{\mathrm{A}}$ is the Alfvén Velocity $\mathbf{v}_{\mathrm{A}} = \mathbf{B}\left(\mu_0\rho\right)^{-\frac{1}{2}}$.

The Kinetic Consistent Scheme

Implementation of magnetic fields is rather difficult due to their pseudo-vector character. Only recently [Chetverushkin et al., 2013],[Chetverushkin et al., 2014] this has been possible by extending the velocity vector $\mathbf{v}$ to the complex plane, $\mathbf{v} \to \mathbf{v} + i\mathbf{v}_{\mathrm{A}}$, where $\mathbf{v}_{\mathrm{A}}$ is the Alfvén Velocity $\mathbf{v}_{\mathrm{A}} = \mathbf{B}\left(\mu_0\rho\right)^{-\frac{1}{2}}$.
The Maxwellian distribution function then becomes

$$f_{\mathrm{M}} = \frac{\rho m^{\frac{1}{2}}}{\left[2k_{\mathrm{B}}T\right]^{\frac{3}{2}}} \exp\left\{-\frac{m}{2k_{\mathrm{B}}T}\left|\boldsymbol{\xi} - \mathbf{v} - i\mathbf{v}_{\mathrm{A}}\right|^2\right\}$$

Implementation of magnetic fields is rather difficult due to their pseudo-vector character. Only recently [Chetverushkin et al., 2013],[Chetverushkin et al., 2014] this has been possible by extending the velocity vector $\mathbf{v}$ to the complex plane, $\mathbf{v} \to \mathbf{v} + i\mathbf{v}_{\mathrm{A}}$, where $\mathbf{v}_{\mathrm{A}}$ is the Alfvén Velocity $\mathbf{v}_{\mathrm{A}} = \mathbf{B}\left(\mu_0 \rho\right)^{-\frac{1}{2}}$.
The Maxwellian distribution function then becomes

$$f_{\mathrm{M}} = \frac{\rho m^{\frac{1}{2}}}{\left[2 k_{\mathrm{B}} T\right]^{\frac{3}{2}}} \exp\left\{-\frac{m}{2 k_{\mathrm{B}} T} \left|\boldsymbol{\xi} - \mathbf{v} - i\mathbf{v}_{\mathrm{A}}\right|^2\right\}$$

The magnetic field may now be obtained using the invariant $m\xi^*$:

$$\mathbf{B}(\mathbf{x}, t) = \frac{\mathfrak{Im} \int m\xi^* f(\mathbf{x}, \boldsymbol{\xi}, t) \mathrm{d}^3\xi}{\mu_0^{1/2}}$$

The Kinetic Consistent Scheme

In a similar way as before also the MHD equations can be obtained (here for ideal MHD), for example:

$$\mathfrak{Im} \int \left\{ m\xi^* \frac{\partial_t f_{\mathrm{M}}(\mathbf{x}, \boldsymbol{\xi}, t) + \boldsymbol{\xi} \cdot \nabla f_{\mathrm{M}}(\mathbf{x}, \boldsymbol{\xi}, t)}{\mu_0^{1/2}} \right\} \mathrm{d}^3\xi = 0$$

$$\rightarrow \partial_t \mathbf{B} + \nabla \times (\mathbf{v} \times \mathbf{B}) = 0$$

In a similar way as before also the MHD equations can be obtained (here for ideal MHD), for example:

$$\mathfrak{Im} \int \left\{ m\xi^* \frac{\partial_t f_{\mathrm{M}}(\mathbf{x}, \boldsymbol{\xi}, t) + \boldsymbol{\xi} \cdot \nabla f_{\mathrm{M}}(\mathbf{x}, \boldsymbol{\xi}, t)}{\mu_0^{1/2}} \right\} \mathrm{d}^3\xi = 0$$

$$\rightarrow \partial_t \mathbf{B} + \nabla \times (\mathbf{v} \times \mathbf{B}) = 0$$

$$\mathfrak{Im} \int \left\{ m \left[\partial_t f_{\mathrm{M}}(\mathbf{x}, \boldsymbol{\xi}, t) + \boldsymbol{\xi} \cdot \nabla f_{\mathrm{M}}(\mathbf{x}, \boldsymbol{\xi}, t) \right] \right\} \mathrm{d}^3\xi = 0 \rightarrow \nabla \cdot \mathbf{B} = 0$$

The Kinetic Consistent Scheme

In a similar way as before also the MHD equations can be obtained (here for ideal MHD), for example:

$$\mathfrak{Im}\int\left\{m\xi^*\frac{\partial_t f_{\mathrm{M}}(\mathbf{x},\boldsymbol{\xi},t)+\boldsymbol{\xi}\cdot\nabla f_{\mathrm{M}}(\mathbf{x},\boldsymbol{\xi},t)}{\mu_0^{1/2}}\right\}\mathrm{d}^3\xi=0$$
$$\rightarrow\partial_t\mathbf{B}+\nabla\times(\mathbf{v}\times\mathbf{B})=0$$

$$\mathfrak{Im}\int\left\{m\left[\partial_t f_{\mathrm{M}}(\mathbf{x},\boldsymbol{\xi},t)+\boldsymbol{\xi}\cdot\nabla f_{\mathrm{M}}(\mathbf{x},\boldsymbol{\xi},t)\right]\right\}\mathrm{d}^3\xi=0\rightarrow\nabla\cdot\mathbf{B}=0$$

The same algorithm as before may be used

Numerical Implementation - Examples

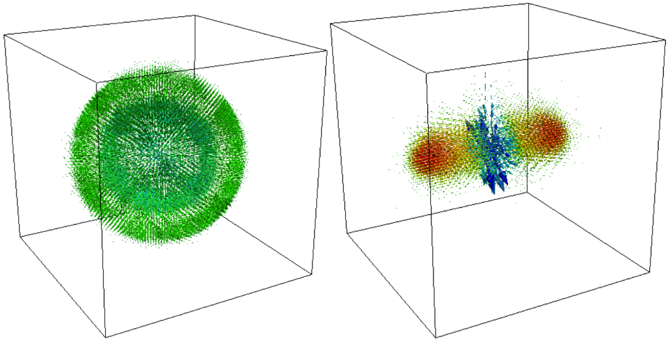

Spherical explosion without and with magnetic field (homogeneous in z-direction) [Chetverushkin et al., 2013]

Application – Sod Test: Magnetic Field (Mass Density)

Application – Sod Test: Magnetic Field (Field Strength)

Conclusions and Outlook

- GRPropa is up and running, ready to be tested especially concerning helicity

Conclusions and Outlook

- GRPropa is up and running, ready to be tested especially concerning helicity
- The expicit semianalytical computation of the backreaction of the magnetic field on the medium gives the result of a power law behavior with $M_q \propto q^4 \propto L^{-4}$ (i.e. $B \propto q^{\frac{5}{2}} \propto L^{-\frac{5}{2}}$) and $U_q \propto q^4 \propto L^{-4}$ and equipartition at large scales.

Conclusions and Outlook

- GRPropa is up and running, ready to be tested especially concerning helicity
- The expicit semianalytical computation of the backreaction of the magnetic field on the medium gives the result of a power law behavior with $M_q \propto q^4 \propto L^{-4}$ (i.e. $B \propto q^{\frac{5}{2}} \propto L^{-\frac{5}{2}}$) and $U_q \propto q^4 \propto L^{-4}$ and equipartition at large scales.
- Helicity enhances this effect by creating an inverse cascade which results in much higher magnetic fields today compared to the non-helical case

Conclusions and Outlook

- GRPropa is up and running, ready to be tested especially concerning helicity
- The expicit semianalytical computation of the backreaction of the magnetic field on the medium gives the result of a power law behavior with $M_q \propto q^4 \propto L^{-4}$ (i.e. $B \propto q^{\frac{5}{2}} \propto L^{-\frac{5}{2}}$) and $U_q \propto q^4 \propto L^{-4}$ and equipartition at large scales.
- Helicity enhances this effect by creating an inverse cascade which results in much higher magnetic fields today compared to the non-helical case
- Kinetic schemes are a powerful and efficient tool to be applied in astrophysics and cosmology, for example in the context of the outflows from galaxies. They have been implemented in a code ready to be tested for different scenarios.

Alves Batista, R., Erdmann, M., Evoli, C., Kampert, K.-H., Kuempel, D., et al. (2013).
CRPropa 3.0 - a Public Framework for Propagating UHE Cosmic Rays through Galactic and Extragalactic Space.

Biermann, L. (1950).
Über den Ursprung der Magnetfelder auf Sternen und im interstellaren Raum (mit einem Anhang von A. Schlüter).
Zeitschrift f. Naturforschung A, 5:65.

Chetverushkin, B., D'Ascenzo, N., and Saveliev, V. (2013).
Novel Kinetic 3D MHD Algorithm for High Performance Parallel Computing Systems.
arXiv, page 1305.0701.

Chetverushkin, B., DâĂŹAscenzo, N., and Saveliev, V. (2014).

Kinetically Consistent Magnetogasdynamics Equations and their Use in Supercomputer Computations.
Dokl. Math., 90(1):495–498.

Chetverushkin, B. N. (2008).
Kinetic Schemes and Quasi-Gas Dynamic System of Equations.
CIMNE, Barcelona.

Dolag, K., Kachelrieß, M., Ostapchenko, S., and Tomàs, R. (2009).
Blazar Halos as Probe for Extragalactic Magnetic Fields and Maximal Acceleration Energy.
Astrophys. J., 703(1):1078.

Junklewitz, H. and Enßlin, T. A. (2011).
Imprints of Magnetic Power and Helicity Spectra on Radio Polarimetry Statistics.
Astron. Astrophys., 530:A88.

Kachelrieß, M., Ostapchenko, S., and Tomàs, R. (2012).
ELMAG: A Monte Carlo Simulation of Electromagnetic Cascades on the Extragalactic Background Light and in Magnetic Fields.

Comp. Phys. Commun., 183:1036–1043.

Neronov, A., Semikoz, D., Kachelrieß, M., Ostapchenko, S., and Elyiv, E. (2010).
Degree-Scale GeV "Jets" from Active and Dead TeV Blazars.
Astrophys. J. Lett., 719(2):L130.

Neronov, A. and Semikoz, D. V. (2009).
Sensitivity of γ-ray Telescopes for Detection of Magnetic Fields in the Intergalactic Medium.
Phys. Rev. D, 80:123012.

Saveliev, A., Jedamzik, K., and Sigl, G. (2012).
Time Evolution of the Large-Scale Tail of Non-Helical Primordial Magnetic Fields with Back-Reaction of the Turbulent Medium.
Phys. Rev. D, 86:103010.

Saveliev, A., Jedamzik, K., and Sigl, G. (2013).
Evolution of Helical Cosmic Magnetic Fields as Predicted by Magnetohydrodynamic Closure Theory.

Phys. Rev. D, 87:123001.

Sigl, G., Olinto, A. V., and Jedamzik, K. (1997).
Primordial Magnetic Fields from Cosmological First Order Phase Transitions.
Phys. Rev. D, 55:4582–4590.

Tashiro, H., Chen, W., Ferrer, F., and Vachaspati, T. (2013).
Search for CP Violating Signature of Intergalactic Magnetic Helicity in the Gamma Ray Sky.
Mon. Not. R. Astron. Soc., 445:L41–L45.

Tashiro, H. and Vachaspati, T. (2013).
Cosmological Magnetic Field Correlators from Blazar Induced Cascade.
Phys. Rev. D, 87:123527.

Turner, M. S. and Widrow, L. M. (1988).
Inflation-Produced, Large-Scale Magnetic Fields.
Phys. Rev. D, 37:2743–2754.

von Kármán, T. and Howarth, L. (1938).
On the Statistical Theory of Isotropic Turbulence.
Proc. R. Soc. London, Ser. A, 164(917):192–215.

Zeldovich, Y. B., Ruzmaikin, D. D., and Sokoloff, D. D. (1980).
Magnetic Fields in Astrophysics.
McGraw-Hill.